A spatially distributed model for the assessment of land use impacts on stream temperature in small urban watersheds

Journal:	*Hydrological Processes*
Manuscript ID:	HYP-13-0889
Wiley - Manuscript type:	Research Article
Date Submitted by the Author:	18-Dec-2013
Complete List of Authors:	SUN, NING; University of Washington, Department of Civil and Environmental Engineering Yearsley, John; University of Washington, Department of Civil and Environmental Engineering Voisin, Nathalie; Pacific Northwest National Laboratory, Hydrology Technical Group Lettenmaier, Dennis; University of Washington, Department of Civil and Environmental Engineering
Keywords:	Stream Temperature Prediction, Riparian Shading, Urban Hydrology, Land Use Change

SCHOLARONE™
Manuscripts

Title: A spatially distributed model for the assessment of land use impacts on stream temperature in small urban watersheds

Ning Sun [a], John Yearsley [a], Nathalie Voisin [b], Dennis Lettenmaier [a]

[a] Department of Civil and Environmental Engineering, University of Washington, Seattle, WA, 98195

[b] Hydrology Technical Group, Pacific Northwest National Laboratory, Richland, WA, 99352

Corresponding Authors:

Dennis Lettenmaier: dennisl@uw.edu

Address: Wilson Ceramic Laboratory, Box 352700, University of Washington, Seattle, WA 98195-2700

Phone: (206) 543-2532

Key Words:

Stream Temperature Prediction, Urban Hydrology, Land Use Change, Riparian Shading

For Peer Review

Abstract

Stream temperatures in urban watersheds are influenced to a high degree by anthropogenic impacts related to changes in landscape, stream channel morphology, and climate. These impacts can occur at small time and length scales, hence require analytical tools that consider the influence of the hydrologic regime, energy fluxes, topography, channel morphology, and near-stream vegetation distribution. Here we describe a modeling system that integrates the Distributed Hydrologic Soil Vegetation Model, DHSVM, with the semi-Lagrangian stream temperature model RBM, which has the capability to simulate the hydrology and water temperature of urban streams at high time and space resolutions, as well as a representation of the effects of riparian shading on stream energetics. We demonstrate the modeling system through application to the Mercer Creek watershed, a small urban catchment near Bellevue, Washington. The results suggest that the model is able both to produce realistic streamflow predictions at fine temporal and spatial scales, and to provide spatially distributed water temperature predictions that are consistent with observations throughout a complex stream network. We use the modeling construct to characterize impacts of land use change and near-stream vegetation change on stream temperature throughout the Mercer Creek system. We then explore the sensitivity of stream temperature to land use changes and modifications in vegetation along the riparian corridor.

For Peer Review

1 Introduction

Stream temperature is a primary indicator of the physical, chemical, and biological health of aquatic ecosystems. Long-term changes in stream temperature typically are driven by anthropogenic impacts on climate, landscape, and stream channel morphology. More specifically, stream temperature is predominantly controlled by a suite of factors including the hydrologic regime, surface energy fluxes, topography, channel morphology, and near-stream vegetation and its spatial distribution (Story et al., 2003).

Heat storage capacity, along with a stream's response to thermal energy inputs and the influence of headwater temperatures are a function of stream velocity and water depth, which are determined by the spatial and temporal variations in the hydrologic regime. Additionally, surface and subsurface runoff moving through stream networks contribute to stream temperature variations, depending on the volume of the source water and the temperature difference between source and receiving stream segments (Webb and Zhang, 1997; Ficklin et al., 2012). Variability in topography (elevation, slope and orientation), channel morphology (width, depth, slope and orientation), along with bankside vegetation characteristics affect the stream surface area available for solar heating and in turn control the in-stream energy and water balances.

Compared with large rivers, these physical control factors generally result in more rapid transient response and greater diurnal variations for stream temperatures in small (and especially urban) streams (Brown, 1969; Hockey et al. 1982). However, it is often the case, particularly in small urban catchments, that long-term, high frequency water temperature observations are not available (Nelson and Palmer, 2007; Webb et al., 2008).

Due to the important role that stream temperature plays in ecosystem function at many levels, a great deal of research has been devoted to developing models for predicting

For Peer Review

water temperature in streams and rivers. Mathematical process models based on the thermal energy budget have been developed that conceptualize river systems as a network of line segments or control volumes such as HEATSOURCE (Boyd and Kasper, 2003), CEQUAL-W2 (Cole and Buchak, 1995), QUAL2K (Chapra et al., 2008) and SNTEMP (Theurer et al., 1984). More recently, spatially distributed models have been developed for large-scale, grid-based systems (Yearsley, 2012; Beek et al., 2012; Wu et al., 2012). However, limited attention has been given to the impacts of urban environments on water temperature or to developing spatially distributed water quality models for watershed analysis at small time and space scales. Examples of research efforts relevant to urban environments and/or small-scale stream segments include models of forested environments (Chen et al., 1998; Sridhar et al., 2004) and mountain streams (Runkel and Chapra, 1993). LeBlanc et al. (1997), Nelson and Palmer (2007), Van Buren et al. (2000) and Herb et al. (2008) modeled thermal pollution in urban environments. These efforts have provided valuable insights into the impacts of climate change, land use and urban development on stream temperatures. However, they are not well-suited to assessing the impacts of extreme events at catchment and watershed scales. This type of assessment requires the ability to perform high-resolution analyses in space and time. Stream thermal behavior along water courses in response to meteorological, hydrological and land use variability generally is highly variable spatially and heterogeneous particularly under conditions of low discharge and strong heating (Webb et al., 2008). Stated otherwise, stream thermal variability is controlled not only by spatial variability in meteorological and hydrological factors, but also by the detailed spatial structure of stream networks (Brown, 1969). Because streamflow measurements are taken at stream gauges which

For Peer Review

represent points along a river network, spatially continuous hydrological measurements rarely exist. Consequently, stream temperature models that rely on streamflow measurements as hydrological inputs have inherent limitations in revealing spatial patterns of stream temperature. As such, an integrated hydrologic/stream-temperature modeling system that accounts for spatial variability in the controlling factors is desirable to predict spatially and temporally continuous temperatures for small streams.

A number of previous studies have developed and assessed coupled hydrological and stream temperature models for applications at different spatial extent. Boyd and Kasper (2003) developed the Heat Source model which contains a one-dimensional hydrological model based on the Saint Venant equation and a reach-scale temperature model. Chen et al. (1998) linked the SHADE program with Hydrologic Simulation Program-Fortran (HSPF) to simulate the dynamic effect of riparian vegetation shading on watershed-scale stream temperature. Krause et al. (2004) combined the reach-scale steady state Stream Network Temperature Model SNTEMP with HSPF (SNTEMP-HSPF) to investigate urbanization impacts on temperature in small streams. Ficklin et al. (2012) developed a stream temperature model within the Soil and Water Assessment Tool (SWAT). All these models conceptualize river systems as a network of line segments and are designed to simulate the temperatures of specific and natural stream segments (Yearsley, 2012). Also, both HSPF and SWAT are semi-distributed hydrologic models, which employ lumped parameterizations within each catchment or hydrologic response unit (HRU). As a result, they have limitations in capturing spatial heterogeneity in land cover and land use and thus are not well suited for high-resolution analyses of small streams.

For Peer Review

In this study, we describe a grid-based modeling system that couples the three-dimensional fully distributed hydrological model DHSVM (Wigmosta et al., 1994) and the spatially distributed stream temperature model RBM (Yearsley, 2009), referred to as DHSVM-RBM, to provide dynamic stream temperature simulations of small urban stream temperature dynamics. DHSVM is particularly well suited to coupling with stream temperature models because (1) it simulates the full water and energy balances at each grid cell that is spatially and hydrologically linked with other grid cells through a detailed channel (and subsurface) flow network. Hence it provides spatially distributed water and energy inputs to the stream temperature model; (2) it uses gridded climate observations as forcings, making it a viable option to extend the application scale of the coupled model to large river systems; (3) RBM uses a grid-based modeling approach that can be readily coupled with DHSVM for modeling stream temperature at small scales.

The grid-based modeling system we describe simulates stream temperatures at hydrologically and spatially linked nodes that aggregate hydrologic and thermal properties in each cell rather than the temperatures of specific stream segments (Yearsley, 2012). The fine-scale spatial variations and patterns in stream temperature that are simulated can be used to infer underlying processes and locate hotspots in a management context. The modeling system allows comprehensive analysis of the temperatures of small stream that reflect physical parameters of the stream environment including, contributing landscape characteristic, surface and sub-surface hydrology, channel morphology, stream geometry, bed properties and near-stream vegetation features. For application to small streams, we have enhanced the DHSVM-RBM model by inclusion of a riparian shading module. We give particular attention to the effect of landscape alterations and riparian vegetation

For Peer Review

shading on stream temperature. The integrated hydrology and stream temperature modeling system explicitly represents both overland surface and subsurface hydrology as well as in-stream heat and mass transfer processes related to stream temperature dynamics. Therefore, historical and future landscape changes at varying degrees resulting from human activities or management practices can be incorporated in the model readily, and we use this capability to evaluate implications of alternative streamside vegetation scenarios in a small urban watershed, Mercer Creek, WA.

The modeling framework allows us to address the following scientific questions:

1) Under current land use and climate condition, what is the effect on stream temperature of current riparian shading in the Mercer Creek watershed?

2) How sensitive is stream temperature to riparian vegetation characteristics including tree height, bank to canopy distance, LAI and buffer width?

3) What has been the effect of land use change and induced changes in streamflow to stream temperature in the Mercer Creek watershed?

4) What are the implications of alternative streamside vegetation scenarios for stream temperature in Mercer Creek?

In order to answer these questions, we carried out a set of experiments using the modeling framework with multiple land cover and riparian shadings scenarios over the Mercer Creek urban watershed, in the greater Seattle, Washington area. The next section describes the coupled modeling framework with the riparian shading enhancement, the study site and model set up. The third section addresses the first and second scientific questions while the fourth section presents the experimental design and results to address the third and fourth questions.

For Peer Review

2 Model development

The DHSVM-RBM modeling system integrates the stream temperature model RBM with the spatially distributed hydrologic model DHSVM to provide dynamic predictions of stream temperature at a high spatial resolution, with a particular interest in small and medium sized urbanized catchments. We describe the model components briefly below.

2.1. The DHSVM hydrology model

DHSVM (Wigmosta et al., 1994) is a physically-based, fully distributed time-continuous hydrological model that mostly has been applied to mountainous watersheds at a high spatial resolution (30 meters to hundreds of meters) to simulate surface and subsurface runoff at sub-daily time steps. Cuo et al. (2008) modified DHSVM and applied it to watersheds with a mix of natural and urbanized landscapes, and Cuo et al. (2009; 2010) applied the model to explore the effects of historic and projected climate and land cover change on the hydrology of the Puget Sound drainage basin, Washington. DHSVM operates on a collection of spatially linked grid cells, each of which employs full water and energy balance solutions. It has been extensively applied in numerous studies on different aspect of hydrology, for example, mountain hydrology (Leung and Wigmosta, 1999; Bowling and Lettenmaier, 2001; Whitaker et al., 2002), urban hydrology under conditions of climate and land cover change (Cuo et al., 2009, 2011), and sediment transport (Doten et al., 2006; Lanini et al., 2009). The input into DHSVM includes sub-daily precipitation, temperature, wind speed, relative humidity, downward shortwave and longwave radiation (both of which typically are indexed to the daily temperature and temperature range using algorithms described by Bohn et al. (2013), and wind speed. The DHSVM module that spatially disaggregates point-based meteorological inputs to the

For Peer Review

model's fine spatial grid explicitly represents the effects of topography on incident and reflected solar radiation.

2.2 The RBM stream temperature model

The RBM stream temperature model uses concepts developed in a basin-wide assessment of water temperatures in the Columbia and Snake river systems (Yearsley, 2009) and in a grid-based approach intended for application to large river systems (Yearsley, 2012; van Vliet et al., 2012) (see Supplementary Section). The computational framework utilizes an Eulerian-Lagrangian particle tracking scheme, which is highly accurate in advection-dominated hydraulic regimes and is inherently stable at large time steps (Manson et al, 2001). The modeling scheme assumes that freshwater systems are well-mixed vertically and laterally. Upstream boundary temperatures are estimated using the method of Mohseni et al. (1998) when no observations are available. The temperature of the subsurface water entering a stream segment is approximated by the average annual air temperature. The water depth and velocity in each stream segment are required to obtain solutions to the semi-Lagrangian thermal energy budget (Sinokrot and Stefan, 1993). We estimated these hydraulic parameters using stage-discharge rating curves derived from monitoring data and relationships described in Chapra (1997) and Leopold and Maddock (1953).

The input data required by RBM include: incoming and outgoing flow to and from each stream segment, downward shortwave and longwave radiation to the channel segment, and air temperature, actual vapor pressure, and wind speed over the channel segment.

For Peer Review

2.3. Coupling of DHSVM with RBM

DHSVM and RBM are coupled in a one-way fashion. DHSVM simulates the energy budget and water balance of each grid cell. A stream network is created in DHSVM based on the DEM map using algorithms described in Wigmosta and Perkins (2001) to define the flow direction and connectivity between channel segments en route to the basin outlet. The extent of the stream network is defined via a specified support area (the area that drains to upstream terminus of each tributary). Streamflow in each channel segment is generated by channel interception of surface and subsurface runoff from the grid cells through which the segment passes. We modified DHSVM so that it aggregates the heat-budget variables required by RBM in all grid cells that intercept a given stream segment using a weighted average based on the length of intercepting stream channel segment.

Topographic effects on shortwave radiation are represented internally in DHSVM. We use the same algorithms to represent solar radiation incident on a channel segment (both direct and diffuse) as related to stream topographic factors (slope and aspect), and solar geometry (altitude and azimuth). First, DHSVM partitions the downward solar radiation into direct and diffuse beams (see supplementary material). Next, DHSVM takes grid elevation, date and time, location of each stream segment as input to calculate the adjusted beam radiation (I'_{direct}) as affected by topographic shading:

$$I'_{direct} = I_{direct} \times [\sin\alpha\cos\varphi\cos(\beta - \theta_{sun}) + \cos\alpha\sin\varphi] \qquad \text{Eq. 1}$$

where α is slope, β is aspect, θ_{sun} is solar azimuth angle, indicating the angle of the position of the sun relative to true north, and φ is solar altitude. A sky view factor based method is applied to compute the topographic shading effect on diffuse solar radiation:

$$I'_{diffuse} = I_{diffuse} \times f_1 \qquad \text{Eq. 2}$$

For Peer Review

where f_1 represents the sky view (ranging from 0 to 1 with a value of 1 indicating a full sky view) obstructed by stream topography. The sky view factor is derived using the method of Rich et al. (1994).

2.4. Riparian vegetation shading effect

To provide RBM with sub-daily input energy budget variables, we developed a new algorithm within DHSVM to take into account the riparian vegetation shading effect on downward solar radiation for channel segment. Downward solar radiation is first partitioned into direct and diffuse beam radiation (see supplemental material). Given riparian vegetation buffers with varying characteristics and stream reaches with different geometries, direct beam radiation can reach the stream through two pathways as illustrated in Fig. 1b: (1) radiation directly reaching the stream without attenuation, labeled I_1, and (2) radiation transmitted through a vegetative buffer of width W_{buffer} (labeled I_2). Both I_1 and I_2 depend on the shadow length cast from the buffer canopy on the stream surface. The method we use to account for the effect of riparian vegetation is adapted from Chen et al. (1998) and Sridhar et al. (2004).

Shadow length of the buffer canopy is estimated as a function of solar altitude (φ) and azimuth (θ_{sun}), and stream azimuth (θ_{stream}) in addition to vegetation height (Fig. 1a):

$$X = (H_{tree} + H_{bank}) \times \left| \frac{\sin(\theta_{sun} - \theta_{stream})}{\tan\varphi} \right| \qquad \text{Eq. 3}$$

where H_{tree} is vegetation height, and H_{bank} is bank height. Shadow length is compared with stream width (W_{stream}) and distance from canopy to bank (D_s). The average path length, λ_{avg}, through the buffer for direct beam radiation depends on whether the stream is fully, partially or not shaded. Assuming the bank height, H_{bank}, is negligible and I_3 is zero, the average path length is estimated as the average of the path lengths associated with the

For Peer Review

direct beams I_1 and I_2 in Figure 1. The path distances of the direct beam radiation components, I_1 and I_2 are determined as one of six different conditions (Table 1), where the horizontal path distances, Δ_1 and Δ_2 of each of the direct bean radiation components, I_1 and I_2 are given by

$$\Delta_1 = (H_{tree} + H_{bank}) \times \left| \frac{\sin(\theta_{sun} - \theta_{stream})}{\tan\varphi} \right| - (H_{bank} + W_{stream}) \quad \text{Eq. 4}$$

$$\Delta_2 = (H_{tree} + H_{bank}) \times \left| \frac{\sin(\theta_{sun} - \theta_{stream})}{\tan\varphi} \right| - W_{stream} \quad \text{Eq. 5}$$

If the stream is shaded, the effective shading width X_{eff} is estimated using Beer's law (Oke, 1978; Monteith and Unsworth, 1990; DeWalle, 2010):

$$X_{eff} = (X - D_s) \times (1 - e^{-\lambda L_{avg}}) \quad \text{Eq. 6}$$

where λ, the extinction coefficient, is estimated as a function of leaf area index (LAI), and L_{avg} is average path length of a sunbeam through vegetation buffer. If the buffer canopy overhangs stream surface, the effective width of stream surface shaded by overhanging canopy is approximated using the method described in Chen et al. (1998). Finally, the net beam radiation reaching the stream surface is computed as:

$$I''_{direct} = I'_{direct} \times \left(1 - \frac{X_{eff}}{W_{stream}}\right) \quad \text{Eq. 7}$$

where I''_{direct} is adjusted direct radiation by topographic shading. The net diffuse solar radiation under riparian vegetation buffer is estimated as a function of the sky view factor adjusted by riparian vegetation buffer if vegetation shade angle (VSA) is greater than topographic shade angle (TSA), as shown in Fig. 1b:

$$I'_{diffuse} = I_{diffuse} \times f_2 = I_{diffuse} \times (1 - 2 \times VSA)$$

For Peer Review

$$VSA = \tan^{-1} \frac{H_{tree} + H_{bank}}{D_s} \qquad \text{Eq. 8}$$

where f_2 represents the view to sky obstructed by riparian vegetation on both sides of the bank.

2.5. Site description and model set up

Mercer Creek, most of the drainage area of which is in the City of Bellevue, Washington, discharges to the Mercer Slough, which eventually drains into Lake Washington (Fig. 2). It has a drainage area of approximately 31 km^2, with elevations ranging from 16 to 326 m. The basin's soils are comprised of 77% hydrological soil group (HSG) C group and 21% of HSG B group, both of which are high runoff potential soil types (SCS, 1986). According to 1990 □ 2012 meteorological records from the Seattle Tacoma International Airport (Sea-Tac) station (112.8 meters, 47°27'N, 122°19'W), which is about 20 km to SW of the centroid of Mercer Creek, the mean annual precipitation is slightly less than 100 cm, the mean annual maximum temperature is about 34°C and the average minimum temperature is about -6°C. Due to urbanization, the Mercer Creek basin has undergone a dramatic landscape alteration over the last century from largely forested to highly urbanized. In 1883, mixed and deciduous forests accounted for nearly 96% of the entire basin with no urban area, whereas the proportion of urbanized area rose up to approximately 82% in 2007, comprised mainly of single-family and multi-family residential areas (Fig. 3; Table 2).

To implement grid-based flow simulations in DHSVM, the basin was subdivided into 71820 grid cells of 30m, each of which was characterized by a suite of parameters associated with topography, soil and vegetation attributes. The spatially linked stream segments comprising the stream network were created based on a digital elevation model

For Peer Review

(DEM) within DHSVM (Fig. 4). Daily records including precipitation, maximum and minimum temperature at the Sea-Tac weather station were obtained from archives of the National Climate Data Center (NCDC), which were then interpolated into hourly gridded precipitation, temperature, downward shortwave and longwave radiation, and wind speeds. Streamflow has been monitored by U.S. Geological Survey (USGS) station 12120000 (47°36'11"N, 122°10'47"W) at the Mercer Creek outlet since 1945. At the same location, stream temperatures were measured once a month from 1977 through 2008. From June 2012 on, temperatures observations were taken at 15-minute intervals at an upstream location (47°37'3"N, 122°9'49"W) corresponding to Seg-37 in Fig. 4.

3. Model validation and effect of riparian shading on stream temperature

3.1 Model evaluation

To evaluate DHSVM-RBM, the model-generated hydrological and temperature predictions were compared with observations at the Mercer Creek outlet. The model run was for the period 2004 through 2012, using 2007 land cover. We employed three statistical criteria to evaluate hydrologic predictions at daily time scale and temperature predictions at the hourly scale, including the Nash-Sutcliffe coefficient (Nash and Sutcliffe, 1970), the modified coefficient of determination using the regression gradient (adjusted R^2) following the method in Krause et al. (2005), and the root mean square error (RMSE). For the first two criteria, a value of 1 indicates a perfect match between model predictions and observations.

Hydrologic evaluation

The results suggest that DHSVM streamflow predictions match observations fairly well at the daily scale (Fig. 5). The Nash-Sutcliffe coefficient over the entire simulation

For Peer Review

period is 0.93, while the adjusted R^2 is 0.87. Summary statistics are also reported for the 1st, 2nd and 3rd quartiles of the flow distribution in Table 3. The lowest streamflow quartile, often corresponding to the highest stream temperature, is reproduced with Nash–Sutcliffe efficiency 0.72, and adjusted R^2 is 0.68.

Stream temperature evaluation

The parameters associated with riparian vegetation were calibrated using stream temperature observations. The calibrated parameters used to represent the existing riparian vegetation include the vegetation height (10m), the buffer width (5m), the LAI (5), and the distance from bank to canopy (0.01m). These parameters were also used to represent the reference condition in the riparian vegetation parameter sensitivity tests. The stream temperature predictions were then compared with observations taken at two locations along Mercer Creek. Fig. 6a shows a scatterplot of instantaneous temperature predictions against 119 temperature observations collected once a month at discrete points in time at the outlet Seg-51. The agreement between observations and predictions is indicated by a Nash-Sutcliffe efficiency of 0.93 and modified R^2 of 0.85. The main discrepancies occur during winter when the model tends to over-predict the temperatures. This may be attributable to the model assumptions of constant inflow groundwater temperature (10°C) and/or stream bed temperature (10°C). Fig. 6b compares the predicted and observed mean diurnal stream temperatures at an upstream reach Seg-37 (observations were aggregated from 15-minute monitoring records). The figure shows a good match between the observations and simulations except that the model tends to under-estimate the temperatures in October and November, which correspond to cold air temperatures and high flows. Model results were further evaluated by comparing predicted and observed

For Peer Review

quartiles of the streamflow distribution (Table 4). The statistical indices suggest a fairly good agreement between the simulations and observations for all flow quartiles. For the lowest streamflow quartile which represents the critical period characterized by low flows and often high temperatures during summer, the Nash-Sutcliffe and modified R^2 are 0.9.

3.2 Riparian shading

The effectiveness of riparian shading is controlled primarily by the relationship between solar and channel geometry in addition to riparian vegetation characteristics. Presumably, sensitivities of riparian vegetation parameters, such as average tree height, bank to canopy distance, LAI, and buffer width could vary with different channel geometries and/or solar distributions. Here we fixed the solar geometry by performing parameter sensitivity test on the stream temperature at noon of July 29th of Year 2009 when the air temperature was at a record high of 39°C. Hence the solar altitude and azimuth are constant 0.96 and 3.3 (in radians), respectively. A sensitivity coefficient was then computed as the ratio of the change in the outputs of interest to the change in a particular parameter compared to a reference or current condition, while the other parameters were held constant (Krieger et al., 1977). To better represent channel geometries in the creek, we selected six main tributaries including the outlet segment seg-51 with varying widths (6□9m) and orientations (40°□ 180°). Sensitivity coefficients were computed for each. A segment index that combines the channel geometry relative to the solar geometry (Eq. 9) was used to characterize each selected segment (Table 5). Two outputs used in the sensitivity tests are: effective shading density λ_{eff} computed as effective shading width (X_{eff}) divided by W_{stream}, and stream temperature at noon of July 29, 2009.

For Peer Review

$$index = \frac{\left|\sin(\theta_{sun} - \theta_{stream})\right|}{W_{stream}} \quad \text{Eq. 9}$$

The tested parameters and sensitivity analysis results are presented in Fig. 9 and Table 6. The results indicated that the sensitivity of all parameters are positively correlated with the channel segment index. In another word, for all parameters, the effective shading density (λ_{eff}) shows the greatest magnitude of change in response to parameter changes for the channel segment with a highest index. An increase in tree height from 0□30 m increases λ_{eff} by 2%□3% per unit tree height; compared with the baseline temperature given tree height of 10 m, stream temperature is decreased by about 0.6□1.9°C across all tested segments if tree height is increased to 30 m. Tree height greater than 30 m, however, has minimal effects (around 0.01°C per unit tree height) on stream temperatures. Across all segments, increasing vegetation buffer width from 0□6 m leads to an increase of λ_{eff} by 2%□10% per unit width; compared with the baseline temperature given width of 5 m, a decrease in width to 2 m raises stream temperature by 0.4□1°C. Increasing buffer width over 6 m has almost no effect on stream temperature for all segments. The sensitivity test on LAI indicates a nearly linear relationship between λ_{eff} and LAI. Increasing LAI from zero (no canopy coverage) to 12 (very dense canopy coverage) results in an increase of λ_{eff} by 1%□6% per unit LAI; compared with baseline temperature for LAI of 5. The stream temperature reduction ranges from 0.8□1.5°C if LAI is increased to 12. Bank to canopy distance is negatively correlated with λ_{eff} and stream temperature. When the canopy was moved closer to the bank from 6□0 m), λ_{eff} was reduced by 1%□6% per unit distance and the temperature was reduced by 1.4□2.2°C.

For Peer Review

4. Coupling land use and riparian vegetation scenarios

We constructed a pre-development land use scenario using the 1883 land cover map, the earliest time for which we could obtain credible land cover data (Alberti et al. 2004). We constructed a post-development scenario using 2007 land cover data. Both land cover data sets were obtained from the University of Washington's Center of Ecology. In 1883, the Mercer Creek basin was almost completely covered by dense stands of large evergreen trees, primarily Douglas fir. Accordingly, the characteristics of the riparian vegetation in 1883, translated into model input, are represented by tree height of 62 m, buffer width of 50 m, LAI of 9 (Thomas and Winner, 2000), and bank to canopy distance of 0.01 m. Between 1883 and 2007, about 82% of forested land had been converted to urban areas. The riparian vegetation in 2007 is characterized by vegetation height 10 m, buffer width 5 m, and LAI 5, characteristic of a temperate zone mixed stand of evergreen and deciduous trees (Asner et al, 2003). These parameter estimates and an assumed distance from bank to canopy of 0.01 m, comprised the parameter set for model calibration in section 3.1. In order to quantify the impact on stream temperature, particularly during summer low flow periods, offered by changes in riparian shading and land use, we conducted experiments based on four combined scenarios with different land cover and riparian shading conditions:

(1) DHSVM-RBM using 2007 land use and 2007 riparian vegetation (the baseline);

(2) DHSVM-RBM using 2007 land use and 1883 riparian vegetation;

(3) DHSVM-RBM using 1883 land use and 2007 riparian vegetation;

(4) DHSVM-RBM using 1883 land use and 1883 riparian vegetation (pristine conditions).

For Peer Review

For all scenarios, DHSVM-RBM was forced with the same historical meteorological forcings (2004-2009), and identical parameters for the hydrologic and stream temperature models (an implicit assumption is that riparian vegetation does not affect streamflow pattern to any substantial extent). By comparing the stream temperature responses of scenarios (1) and (2), and (3) paired with (4), we focus on the impact of riparian vegetation in 2007 relative to 1883 with no change of streamflow patterns given the same land use scenario. Comparing (1) with (3), we focus on the effect of land use alteration on streamflows, and its consequent effect coupled with more current 2007 riparian vegetation scenario on stream temperature. Stated otherwise, we evaluate the efficiency of the current riparian shading relative to land cover change over the last century on changes in stream temperature. Likewise, comparison of scenarios (2) and (4) allows evaluation of the optimal level of mitigation on stream temperature change due to land use change effect (i.e. change in flow) provided by 1883 riparian shading.

4.1 Land use change effect on streamflow

The comparison of streamflow between pre- (1883) and post-development (2007) land use scenarios suggests that an increase in urbanized area leads to higher mean monthly flows with greater inter-monthly variability over the entire simulation period (Fig 7). The streamflow increase under post-development conditions can be explained by the 82% forest loss that contributes to high mass losses through evapotranspiration (ET) in summer, and reduced soil moisture storage from reduced infiltration as a result of increased impervious areas. This is consistent with the findings of Cuo et al. (2009) for a different (but similarly urbanized) catchment in the same region and is also similar to analyses on the effect of clear cutting forest in the Pacific Northwest region using

For Peer Review

DHSVM (VanShaar et al. 2002, Bowling et al. 2000, Storck et al. 1998). At the daily time scale, both peak flows and baseflows during summer increase post-development (Figure 8). The average summer baseflow is 0.07m^3/s for pre-development and 0.16m^3/s for post-development. The increase in summer baseflow can be explained by significantly reduced ET loss that more than compensates for reduced infiltration caused by the increase in impervious surfaces. In summary, relative to the pre-development scenario, total ET is reduced by 77% post-development while the total outflow increases by 132% in the post-development scenario.

4.2 Stream temperature response to coupled scenarios

The stream temperature response to the four sets of coupled land use and riparian vegetation scenarios, as illustrated above, was compared in terms of average peak temperature. For each year from 2004 through 2009, the average peak temperature was computed as the mean value of the ten highest daily maximum temperatures over the year (Table 7).With identical streamflow characteristics given the post-development land cover but different riparian vegetation scenarios, the comparison between scenario (1) and (2) shows that, compared with the 2007 riparian vegetation scenario, the riparian shading provided by large trees in dense stands over a wide buffer in the 1883 riparian scenario was able to decrease the overall average peak stream by about 4°C. Comparisons between scenarios (3) and (4) yield essentially the same result: the 1883 riparian scenario leads to a decrease of 4°C in overall peak stream temperature when the streamflow patterns of both scenarios are controlled by the 1883 land use scenario. Although scenarios (1) and (3) both have the 2007 riparian shading scenario, they differ in the basin land use scenarios and resulting streamflow characteristics. However, comparison between scenarios (1) and

For Peer Review

(3) indicates almost no effect of streamflow change or land use change on average peak stream temperature; it is nearly identical to the results of comparisons between scenarios (2) and (4). Finally, comparing scenarios (2) and (3) indicates the same magnitude of mean peak temperature reduction (about 4°C) as in the scenario with identical streamflow characteristics but different riparian vegetation conditions, e.g. scenario (1) vs. (2), and scenario (3) vs. (4).

We further compared the effect of the four scenarios on three additional temperatures indicators: annual average temperature, average daily temperature and daily temperature variability during summer months (Table 8). The results suggest that land use change from 1883 to 2007, when coupled with the same riparian shading scenario (either 1883 or 2007), has minimal effect on all three temperature indicators. Compared to the 2007 riparian scenario, the 1883 riparian shading with post-development flows results in a decrease in average annual stream temperature of 0.7°C, an average summer daily temperature decrease of 1.1°C, and a reduction in daily temperature variability during the summer months of 0.3□0.4°C.

5. Discussion

We examined the coupled effect of urbanization and riparian vegetation buffers on stream temperature in a rapidly urbanizing catchment and evaluated their relative importance to stream temperature change. With about 82% of forest land converted to urban areas in the pre- to post-development land use transition, both peak flows and baseflow increased throughout the year. However, we found that changes in flow characteristics had minimal effect on peak stream temperatures, under the same riparian vegetation scenario. In contrast, average peak stream temperature generally decreased by

For Peer Review

about 4°C when current riparian vegetation was replaced by pre-development riparian vegetation. On one hand, as a result of a greater summer baseflow in the post-development land use scenario, stream temperatures tended to be less responsive to energy input. On the other hand, the downward solar radiation plays such an important role in the thermal energy budget that the impact of increased streamflow was overcome by the reduction of downward solar radiation due to the amount of shading provided by the riparian vegetation buffer for both 2007 and 1883 conditions. In other words, the riparian shading offered by vegetation buffers overrides the land use change effect on stream temperature.

We performed a series of sensitivity tests to understanding the relationships between riparian shading and stream temperature. The key findings from the sensitivity analyses are (1) riparian shading is an effective means of modulating stream temperatures. In the case of Mercer Creek, riparian vegetation buffers with tree heights of 30 m, buffer widths of 8 m, canopy to bank distance of 0.01 m and LAI of 9 (e.g. Douglas fir), could make a marked reduction in stream temperature (by about 3°C) compared to current (baseline) conditions at the Mercer Creek mouth (seg-51). Given that the average peak stream temperature for pre-development land use and riparian scenarios (1883□1883) was approximately 4°C lower than the current scenario (2007-2007) at seg-51, it is reasonable to conclude that an efficient riparian buffer design could restore the stream temperature to its "pristine state" as illustrated in pre-development land use and riparian vegetation conditions; (2) The effective range of riparian vegetation parameters showed a strong correlation with the channel segment index that represents channel geometry (consisting of channel orientation and width) relative to solar geometry; and the effectiveness of riparian shading is correlated with the segment index. As a result, the index can be used as

For Peer Review

a basis for determining appropriate and efficient riparian buffer system for a particular stream.

Owing to the grid-based spatial inputs and routing scheme of DHSVM, DHSVM-RBM is able to derive spatially continuous thermal maps throughout a complex stream network. This is important because stream temperature is notably variable along stream gradients (Fig. 10). As spatial variability is inherent to climate and land use change, it is necessary to incorporate spatial variability in future stream temperature scenario modeling to better understanding the basin-wide spatial correlation between stream temperature and landscape/climate change. Climate change scenarios on stream temperature are not discussed in this study because we focus on simulating hydrology and water temperature in small urban catchments with a high resolution in time and space. As we extend model applications to regional scale river systems, such as the Puget Sound basin, downscaled climate change scenarios along with land use change scenarios will need to be applied to examine the climate and land use change effect on regional scale stream temperature.

6. Conclusions

Our grid-based modeling system dynamically couples the spatially distributed hydrologic model and the RBM stream temperature model. It facilitates characterization of the impacts of climate, landscape, and near-stream vegetation changes on stream temperature, and allows modeling of long-term spatially distributed water temperature throughout complex stream networks. Comparisons between simulated and observed streamflow and stream temperature indicate that the model is able to (1) produce reasonable streamflow predictions at fine temporal and spatial scales; (2) provide spatially distributed water temperature predictions that mostly agree with observations throughout

For Peer Review

complex stream network, and (3) characterize impacts of land use change and near-stream vegetation change on stream temperature at local and regional scales in urban environments.

As applied to the small Mercer Creek urban watershed in the Greater Seattle area, our results show that notwithstanding general warming due to climate change over the last century, which has resulted in somewhat warmer stream temperatures (Schindler et al. 1996), there have been concurrent increases in low flows due to urbanization and deforestation, which more or less offset the effects of a warmer climate. On the other hand, loss of riparian vegetation has had a much larger impact in increasing stream temperature and annual maximum stream temperature (around 4°C), which could be mostly reversed by restoring riparian vegetation in a fairly narrow corridor – a finding that has important implications for vegetation management in the riparian corridor. Our findings also emphasize the necessity of representing riparian shading in assessing the impacts of climate and land cover change on urban streams.

Acknowledgements

The research on which this paper is based was funded by U.S. Environmental Protection Agency Science to Achieve Results (STAR) grant No. R835195 to the University of Washington. The authors gratefully acknowledge the assistance of the Hydrologic Services Group of King County, the Utilities Department of the City of Bellevue, and the U.S. Geological Survey which provided observations used herein.

For Peer Review

References

Alberti M, Weeks R, Coe S. 2004. Urban land cover change analysis in Central Puget Sound. *Photogrammetric Engineering and Remote Sensing* **70**: 1043-52.

Asner GP, Scurlock JM, Hicke JA. 2003. Global synthesis of leaf area index observations: implications for ecological and remote sensing studies. *Global Ecology and Biogeography* **12**: 191-205.

Beek LP, Eikelboom T, Vliet MT, Bierkens MF. 2012. A physically based model of global freshwater surface temperature. *Water Resources Research* **48**.

Bohn TJ, Livneh B, Oyler JW, Running SW, Nijssen B, Lettenmaier DP. 2013. Global evaluation of MTCLIM and related algorithms for forcing of ecological and hydrological models. *Agricultural and Forest Meteorology* **176**: 38-49.

Bowling LC, Lettenmaier DP. 2001. The effects of forest roads and harvest on catchment hydrology in a mountainous maritime environment. *Land use and watersheds: Human influence on hydrology and geomorphology in urban and forest areas*: 145-64.

Bowling LC, Storck P, Lettenmaier DP. 2000. Hydrologic effects of logging in western Washington, United States. *Water Resources Research* **36**: 3223-40.

Boyd M, Kasper B. 2003. Analytical methods for dynamic open channel heat and mass transfer: Methodology for heat source model version 7.0. *Oregon Department of Environmental Quality, Portland, Oregon*.

Brown GW. 1969. Predicting temperatures of small streams. *Water Resources Research* **5**: 68-75.

Chapra SC, Pelletier GJ, Tao H. 2008. QUAL2K: A modeling framework for simulating river and stream water quality, version 2.11: Documentation and users manual.

Chapra SC. 1997. *Surface water-quality modeling*. McGraw-Hill New York.

Chen YD, Carsel RF, McCutcheon SC, Nutter WL. 1998. Stream temperature simulation of forested riparian areas: I. Watershed-scale model development. *Journal of Environmental Engineering* **124**: 304-15.

Cole TM, Buchak E. 1995. CE-QUAL-W2: A two-dimensional, laterally averaged, hydrodynamic and water quality model, version 2.0.

Cuo L, Beyene TK, Voisin N, Su F, Lettenmaier DP, Alberti M, Richey JE. 2011. Effects of mid-twenty-first century climate and land cover change on the hydrology of the Puget Sound basin, Washington. *Hydrological Processes* **25**: 1729-53.

For Peer Review

Cuo L, Lettenmaier DP, Alberti M, Richey JE. 2009. Effects of a century of land cover and climate change on the hydrology of the Puget Sound basin. *Hydrological Processes* **23**: 907-33.

Cuo L, Lettenmaier DP, Mattheussen BV, Storck P, Wiley M. 2008. Hydrologic prediction for urban watersheds with the Distributed Hydrology–Soil–Vegetation Model. *Hydrological Processes* **22**: 4205-13.

DeWalle DR. 2010. Modeling Stream Shade: Riparian Buffer Height and Density as Important as Buffer Width1.*JAWRA Journal of the American Water Resources Association* **46**: 323-33.

Doten CO, Bowling LC, Lanini JS, Maurer EP, Lettenmaier DP. 2006. A spatially distributed model for the dynamic prediction of sediment erosion and transport in mountainous forested watersheds. *Water Resources Research* **42**.

Erbs D, Klein S, Duffie J. 1982. Estimation of the diffuse radiation fraction for hourly, daily and monthly-average global radiation. *Solar Energy* **28**: 293-302.

Ficklin DL, Luo Y, Stewart IT, Maurer EP. 2012. Development and application of a hydroclimatological stream temperature model within the Soil and Water Assessment Tool. *Water Resources Research* **48**.

Herb WR, Janke B, Mohseni O, Stefan HG. 2008. Thermal pollution of streams by runoff from paved surfaces. *Hydrological Processes* **22**: 987-99.

Hockey J, Owens I, Tapper N. 1982. Empirical and theoretical models to isolate the effect of discharge on summer water temperatures in the Hurunui River. *Journal of Hydrology (New Zealand)* **21**: 1-12.

Jobson HE, Schoellhamer DH. 1993. *Users manual for a branched Lagrangian transport model*. US Geological Survey.

Krause CW, Lockard B, Newcomb TJ, Kibler D, Lohani V, Orth DJ. 2004. Predicting influences of urban development on thermal habitat in a warm water stream. *JAWRA Journal of the American Water Resources Association* **40**: 1645-58.

Krause P, Boyle D, Bäse F. 2005. Comparison of different efficiency criteria for hydrological model assessment. *Advances in Geosciences* **5**: 89-97.

Krieger, T, Durston, C, Albright, D. 1978. Statistical determination of effective variables in sensitivity analysis. *Trans. Am. Nucl. Soc.* **28**.

For Peer Review

Lanini JS, Clark EA, Lettenmaier DP. 2009. Effects of fire-precipitation timing and regime on post-fire sediment delivery in Pacific Northwest forests. *Geophysical Research Letters* **36**.

LeBlanc RT, Brown RD, FitzGibbon JE. 1997. Modeling the effects of land use change on the water temperature in unregulated urban streams. *Journal of environmental management* **49**: 445-69.

Leopold LB, Maddock T. 1953. The Hydraulic Geometry of Stream Channels and Some Physiographic Implications.

Leung LR, Wigmosta MS. 1999. POTENTIAL CLIMATE CHANGE IMPACTS ON MOUNTAIN WATERSHEDS IN THE PACIFIC NORTHWEST1. *JAWRA Journal of the American Water Resources Association* **35**: 1463-71.

Manson JR, Wallis SG, Hope D. 2001. A conservative semi-Lagrangian transport model for rivers with transient storage zones. *Water Resources Research* **37**: 3321-9.

Mohseni O, Stefan HG, Erickson TR. 1998. A nonlinear regression model for weekly stream temperatures. *Water Resources Research* **34**: 2685-92.

Monteith JL, Unsworth MH. 1990. *Principles of environmental physics*. Edward Arnold, London, United Kingdom.

Nash JE, Sutcliffe JV. 1970. River flow forecasting through conceptual models part I—A discussion of principles. *Journal of hydrology* **10**: 282-90.

Nelson KC, Palmer MA. 2007. Stream temperature surges under urbanization and climate change: Data, models, and responses. *JAWRA Journal of the American Water Resources Association* **43**: 440-52.

Oke TR. 1978. *Boundary layer climates*. Methuen & Co. Ltd.

Rich P, Dubayah R, Hetrick W, Saving S. 1994. Using viewshed models to calculate intercepted solar radiation: applications in ecology. American Society for Photogrammetry and Remote Sensing Technical Papers.

Runkel RL, Chapra SC. 1993. An efficient numerical solution of the transient storage equations for solute transport in small streams. *Water Resources Research* **29**: 211-5.

Schindler DW, Bayley SE, Parker BR, Beaty K, Cruikshank D, Fee E, Schindler E, Stainton M. 1996. The effects of climatic warming on the properties of boreal lakes and streams at the Experimental Lakes Area. *Limnology and Oceanography* **41**: 1004-17.

For Peer Review

Sinokrot BA, Stefan HG. 1993. Stream temperature dynamics: measurements and modeling. *Water Resources Research* **29**: 2299-312.

Soil Conservation Service (SCS). 1986. Technical release 55: urban hydrology for small watersheds.

Sridhar V, Sansone AL, LaMarche J, Dubin T, Lettenmaier DP. 2004. Prediction of stream temperature in forested watersheds. *JAWRA Journal of the American Water Resources Association* **40**: 197-213.

Storck P, Bowling L, Wetherbee P, Lettenmaier D. 1998. Application of a GIS-based distributed hydrology model for prediction of forest harvest effects on peak stream flow in the Pacific Northwest. *Hydrological Processes* **12**: 889-904.

Story A, Moore RD, Macdonald JS. 2003. Stream temperatures in two shaded reaches below cut blocks and logging roads: downstream cooling linked to subsurface hydrology**.** *Canadian Journal of Forest Research* **33**: 1383-96.

Theurer FD, Voos KA, Miller WJ. 1984. *Instream water temperature model*. Western Energy and Land Use Team, Division of Biological Services, Research and Development, Fish and Wildlife Service, US Department of the Interior.

Thomas SC, Winner WE. 2000. Leaf area index of an old-growth Douglas-fir forest estimated from direct structural measurements in the canopy. *Canadian Journal of Forest Research* **30**: 1922-30.

Van Buren M, Watt WE, Marsalek J, Anderson B. 2000. Thermal enhancement of stormwater runoff by paved surfaces. *Water research* **34**: 1359-71.

van Vliet MTH, Yearsley JR, Franssen WHP, Ludwig F, Haddeland I, Lettenmaier DP, Kabat P. 2012. Coupled daily streamflow and water temperature modelling in large river basins. *Hydrology and Earth System Sciences Discussions* **9**: 8335-74.

VanShaar JR, Haddeland I, Lettenmaier DP. 2002. Effects of land-cover changes on the hydrological response of interior Columbia River basin forested catchments. *Hydrological Processes* **16**: 2499-520.

Webb BW, Hannah DM, Moore RD, Brown LE, Nobilis F. 2008. Recent advances in stream and river temperature research. *Hydrological Processes* **22**: 902-18.

Webb B, Zhang Y. 1997. Spatial and seasonal variability in the components of the river heat budget. *Hydrological Processes* **11**: 79-101.

Whitaker A, Alila Y, Beckers J, Toews D. 2002. Evaluating peak flow sensitivity to clear-cutting in different elevation bands of a snowmelt-dominated mountainous catchment. *Water Resources Research* **38**: 1172.

For Peer Review

Wigmosta MS, Vail LW, Lettenmaier DP. 1994. A distributed hydrology-vegetation model for complex terrain. *Water Resources Research* **30**: 1665-79.

Wigmosta MS, Perkins WA. 2001. *Simulating the effects of forest roads on watershed hydrology*, in: Influence of Urban and Forest Land Use on the Hydrologic Geomorphic Responses of Watersheds, edited by: Wigmosta,M. S. and Burges, S. J., AGU Water Science and Application Series.

Wu H, Kimball JS, Elsner MM, Mantua N, Adler RF, Stanford J. 2012. Projected climate change impacts on the hydrology and temperature of Pacific Northwest rivers. *Water Resources Research* **48**.

Yearsley J. 2009. A semi-Lagrangian water temperature model for advection-dominated river systems. *Water Resources Research* **45**.

Yearsley J. 2012. A grid-based approach for simulating stream temperature. *Water Resources Research* **48**.

For Peer Review

Table 1. Conditions determining average path length of direct beam radiation through the riparian vegetation buffer. W_{buffer} is vegetation buffer width, Φ_{solar} is defined as: $\cos(\varphi)*|\sin(\theta_{su} - \theta_{st})|$. Other symbols are defined in Eqs. (5□7) and Figure 1. The conditions use standard C language notation (&& - and, || - or, <= less than or equal to, >= equal to or greater than)

Case	Description	Condition	Average Path, L_{avg}
1	No shade	$\Delta_1 = < 0$ && $\Delta_2 <= 0.0$	0.0
2	Partial shade, sun above buffer canopy	$\Delta_1 <= 0.0$ && $\Delta_2 <= W_{buffer}$	$0.5 * \Delta_2/\Phi_{solar}$
3	Partial shade, sun below buffer canopy	$\Delta_1 <= 0.0$ && $\Delta_2 > W_{buffer}$	$0.5 * W_{buffer}/\Phi_{solar}$
4	Full shade, sun above buffer canopy	$\Delta_1 > 0.0$ && $\Delta_2 <= W_{buffer}$	$0.5*(\Delta_{1+} \Delta_2)/\Phi_{solar}$
5	Full shade, sun partially below buffer canopy	$\Delta_1 <= W_{buffer}$ && $\Delta_2 > W_{buffer}$	$0.5*(\Delta_{1+} W_{buffer})/\Phi_{solar}$
6	Full shade, sun entirely below buffer canopy	$\Delta_1 > W_{buffer}$ && $\Delta_2 > W_{buffer}$	W_{buffer}/Φ_{solar}

For Peer Review

Table 2 Summary of land cover characteristics in 1883 and 2007 in the Mercer Creek

Land Use	**Percentage**	
	1883	2007
Dense Urban	0.0%	24.1%
Light-Medium Urban	0.0%	58.2%
Grass/Crops/Shrubs	0.0%	3.9%
Mixed/Deciduous Forests	95.9%	6.7%
Coniferous Forests	0.0%	5.6%
Wetlands	0.0%	0.5%
Water	4.1%	1.0%

For Peer Review

Table 3 Summary of model performance in streamflow predictions, 2004 □ 2012

Streamflow	Obs. Avg. (m^3/s)	Nash-Sutcliffe	Modified R^2	RMSE (m^3/s)
1st Quartile	0.18	0.72	0.68	0.017
2nd Quartile	0.29	0.66	0.61	0.027
3rd Quartile	1.03	0.91	0.89	0.44

For Peer Review

Table 4 Summary of model performance in mean daily temperature predictions

Streamflow	Obs. Avg. (°C)	Nash-Sutcliffe	Modified R^2	RMSE (°C)
1st Quartile	15.28	0.9	0.89	0.36
2nd Quartile	14.57	0.93	0.9	0.46
3rd Quartile	11.64	0.94	0.94	0.78

For Peer Review

Table 5 Selected channel segments for parameter sensitivity test

Stream Id	length (m)	stream width (m)	stream azimuth (degree)	stream azimuth (radian)	index
33	14.4	6	45	0.8	0.136
36	13.5	9	42.5	0.7	0.088
37	22.3	6	123.7	2.2	0.12
40	11.6	6	160.9	2.8	0.026
51	24.5	9	95.2	1.7	0.1
64	3.9	6	180	3.1	0.029

For Peer Review

Table 6 Stream temperature change from parameter sensitivity tests

Parameters			Stream Temperature Change (°C)					
			seg-33 (*0.136)	seg-37 (*0.12)	**seg-51** (*0.1)	seg-36 (*0.088)	seg-64 (*0.029)	seg-40 (*0.026)
Baseline: **(1)** Tree Height (10) **(2)** Bank to Canopy Dist. (0.01) **(3)** LAI (5) **(4)** Buffer Width (5)	Tree Height (m)	5	0.8	1.2	1.2	0.9	1.1	0.7
		20	-1.1	-1.0	-1.6	-0.5	-0.6	-0.7
		30	-1.9	-1.2	-1.8	-0.6	-0.7	-1.1
		40	-2.1	-1.4	-1.9	-0.7	-0.8	-1.3
		50	-2.2	-1.7	-2.0	-0.8	-0.9	-1.4
		60	-2.4	-1.7	**-2.0**	-0.9	-1.0	-1.5
	Bank to Canopy Dist. (m)	1	0.6	0.6	0.4	0.3	0.3	0.4
		2	0.8	1.1	0.8	0.6	0.9	0.6
		3	1.1	1.4	1.2	1.0	1.3	0.8
		4	1.3	1.6	1.6	1.3	1.7	1.1
		5	1.5	1.9	1.9	1.7	2.0	1.3
		6	1.6	2.1	**2.1**	1.9	2.2	1.4
	LAI	0	1.4	2.1	1.9	1.8	2.1	1.3
		3	0.6	0.9	0.9	0.8	0.9	0.6
		6	-0.2	-0.4	-0.4	-0.3	-0.4	-0.2
		9	-0.6	-1.0	-1.0	-0.8	-0.9	-0.6
		12	-0.8	-1.5	**-1.5**	-1.2	-1.3	-0.9
	Buffer Width (m)	2	0.4	0.8	1.0	0.8	0.9	0.4
		4	0.1	0.1	0.3	0.2	0.2	0.1
		6	0.0	-0.1	-0.2	-0.1	-0.2	-0.1
		8	-0.1	-0.3	-0.5	-0.3	-0.2	-0.3
		10	-0.1	-0.4	**-0.6**	-0.4	-0.3	-0.3

*Note: The temperature change is computed as the difference between the stream temperature of the baseline condition and stream temperature resulting from riparian vegetation parameter change. * indicates the index of channel segments. The segment IDs are sorted in a descending order based on their index.*

For Peer Review

Table 7 Summary of annual mean peak stream temperatures from 2004□2009 under different scenarios

Avg. Peak	Scenario 1 2007-2007	Scenario 2 2007-1883	Scenario 3 1883-2007	Scenario 4 1883-1883
2004	21.43	17.20	21.48	17.17
2005	21.18	17.00	21.29	16.95
2006	21.63	17.41	21.67	17.38
2007	20.97	16.66	21.01	16.64
2008	21.12	17.12	21.17	17.08
2009	21.95	17.83	22.04	17.79
Overall avg.	**21.38**	**17.20**	**21.44**	**17.17**

For Peer Review

Table 8 Summary of annual mean peak stream temperatures from 2004□2009 under different scenarios

	Scenario 1 2007-2007	Scenario 2 2007-1883	Scenario 3 1883-2007	Scenario 4 1883-1883
Annual Avg. Temp.	10.76	10.05	10.78	10.05
Summer Daily Avg. Temp.	15.13	14.05	15.11	14
Summer Daily Temp. stdev	1.61	1.26	1.59	1.24

For Peer Review

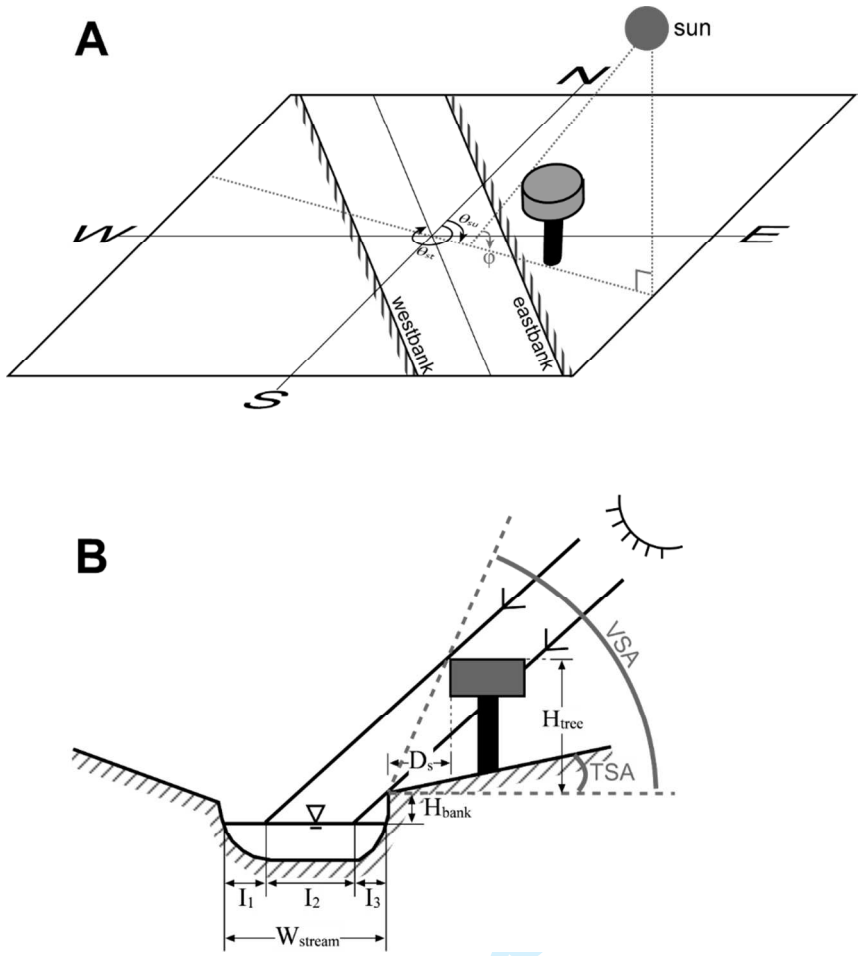

Fig. 1 Schematic of riparian vegetation shading over stream surface. (A) A 3-D view, in which θ_{su} is solar azimuth, θ_{st} is stream azimuth, and φ is solar altitude. (B) A cross-sectional view, in which I_1 represents the length of the stream segment that receives direct radiation, I_2 is the length of the segment that receives radiation attenuated by the canopy, and I_3 is fully shaded. *VSA* is vegetation shade angle and *TSA* is topographic shade angle. H_{tree} and H_{bank} are vegetation and bank height, as defined in Eq. 5□6, respectively. D_s is canopy to bank distance, as defined in Eq. 7

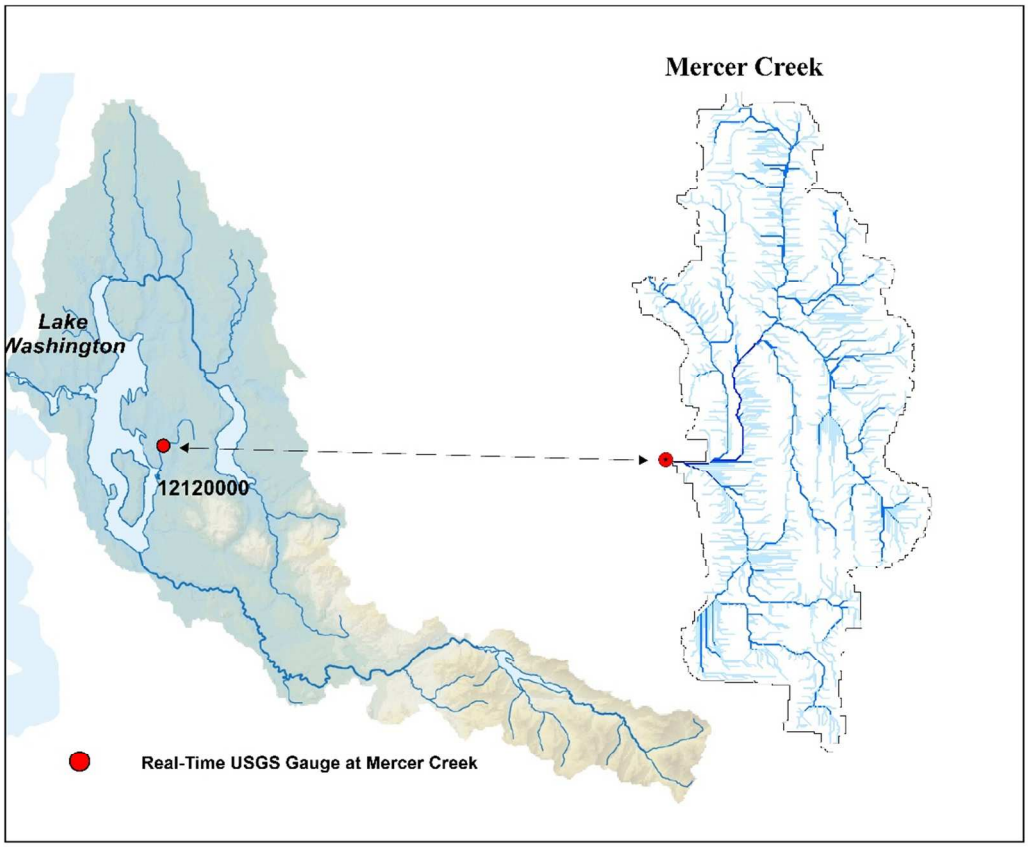

Fig. 2 The Mercer Creek watershed near Bellevue, Washington

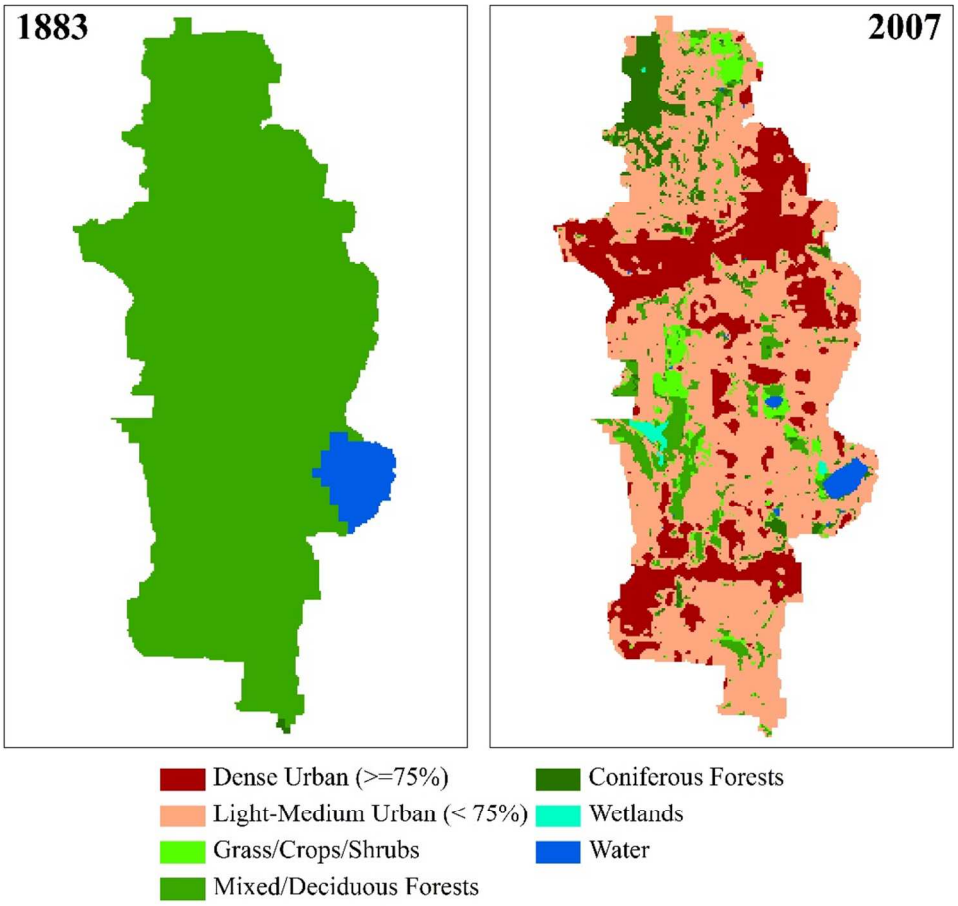

Fig. 3 Mercer Creek land cover maps in Year 1883 and 2007 under the same land cover classification scheme

Review

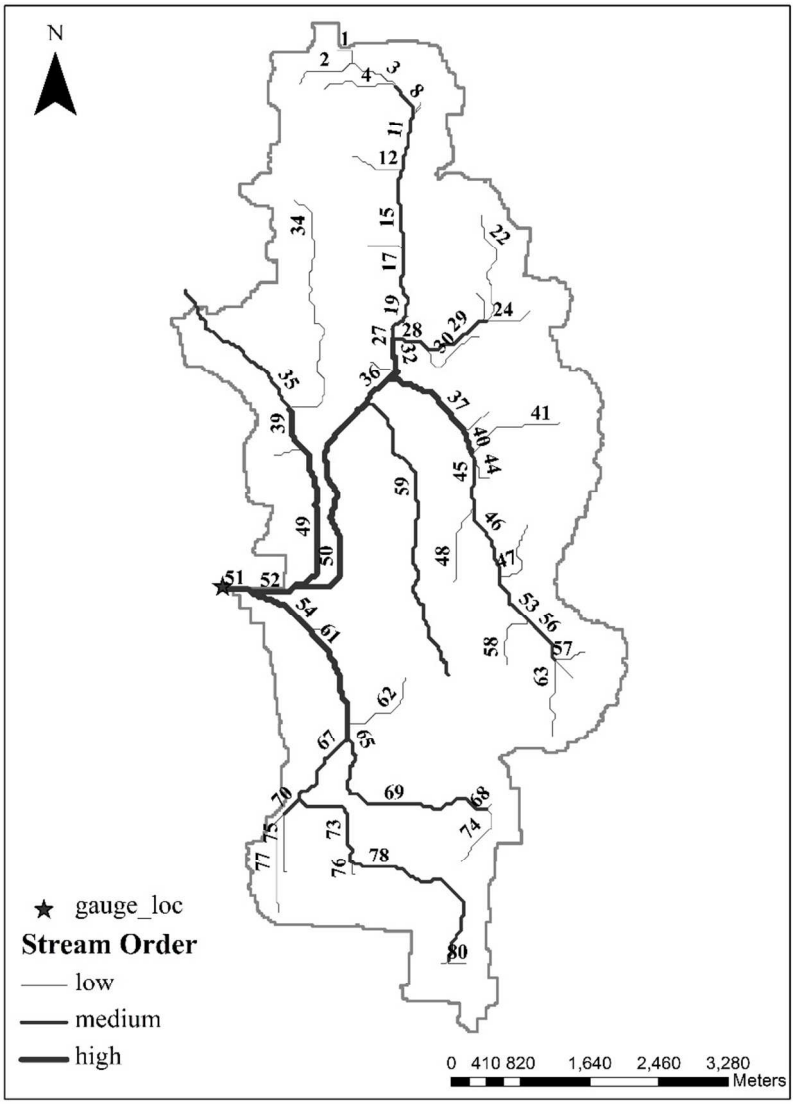

Fig. 4 Mercer Creek stream network labelled with segment IDs

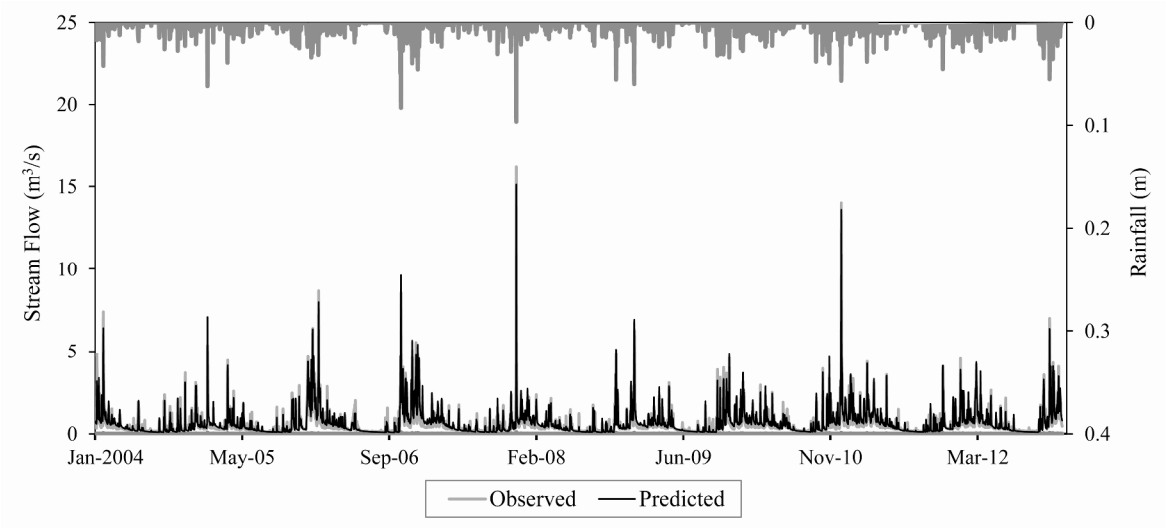

Fig. 5 Comparison between predicted and observed daily hydrographs, 2004 □ 2012 at the Mercer Creek outlet

For Peer Review

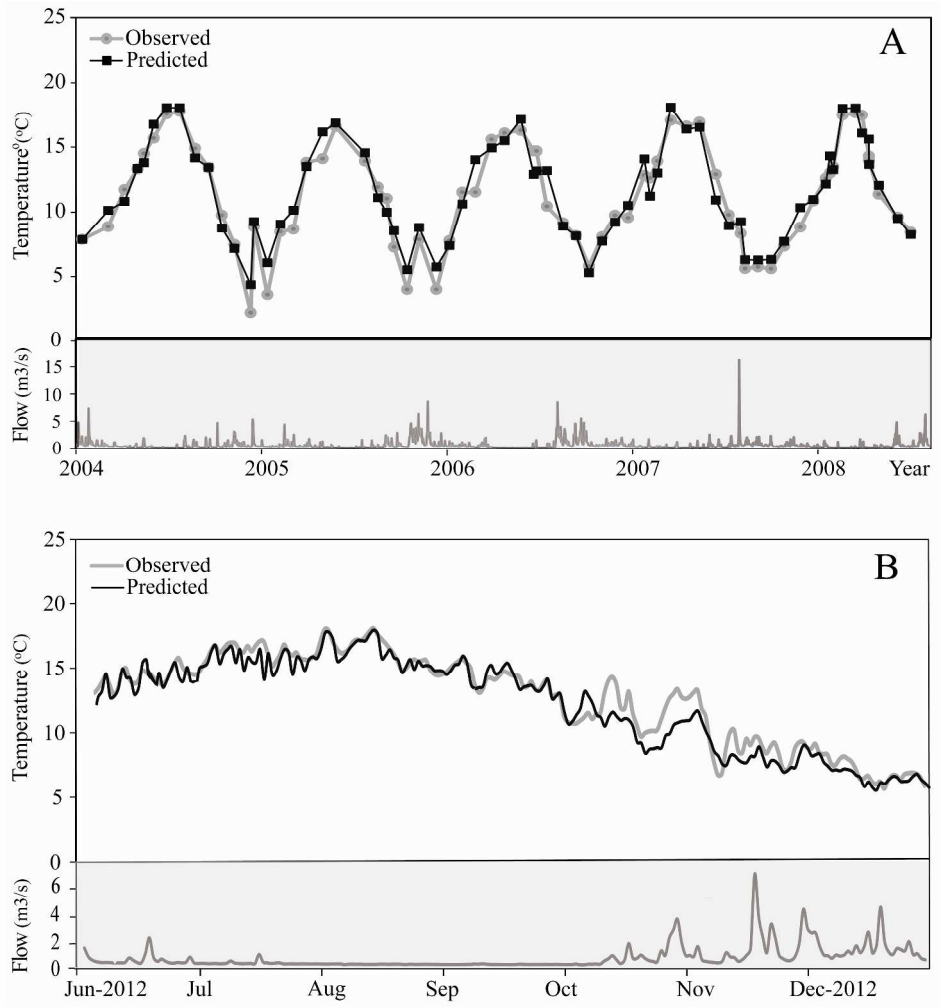

Fig. 6 (A) Instantaneous temperature predictions against observations at the Mercer Creek outlet (Seg-51); (B) mean diurnal daily observation against prediction at an upstream reach of Mercer Creek (Seg-37). In each figure, the observed hydrograph is shown in the lower graph.

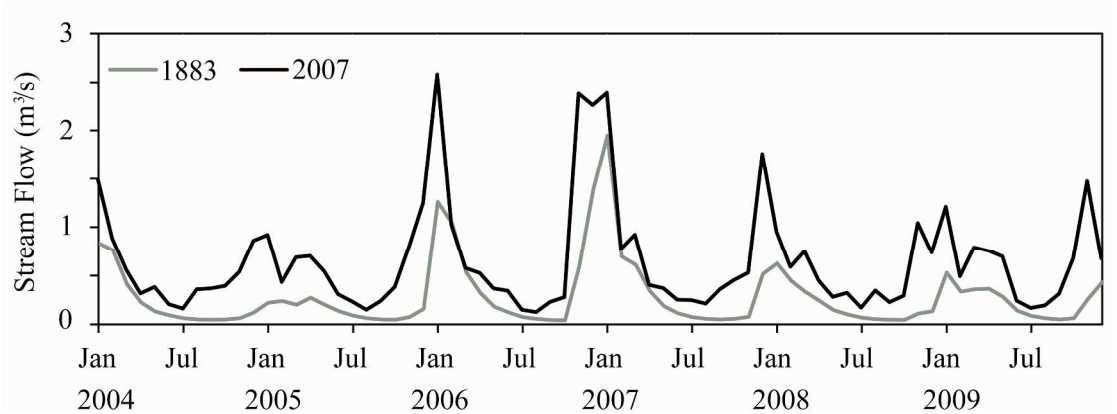

Fig. 7 Comparison of monthly mean streamflow between pre- (1883) and post-development (2007) scenarios

For Peer Review

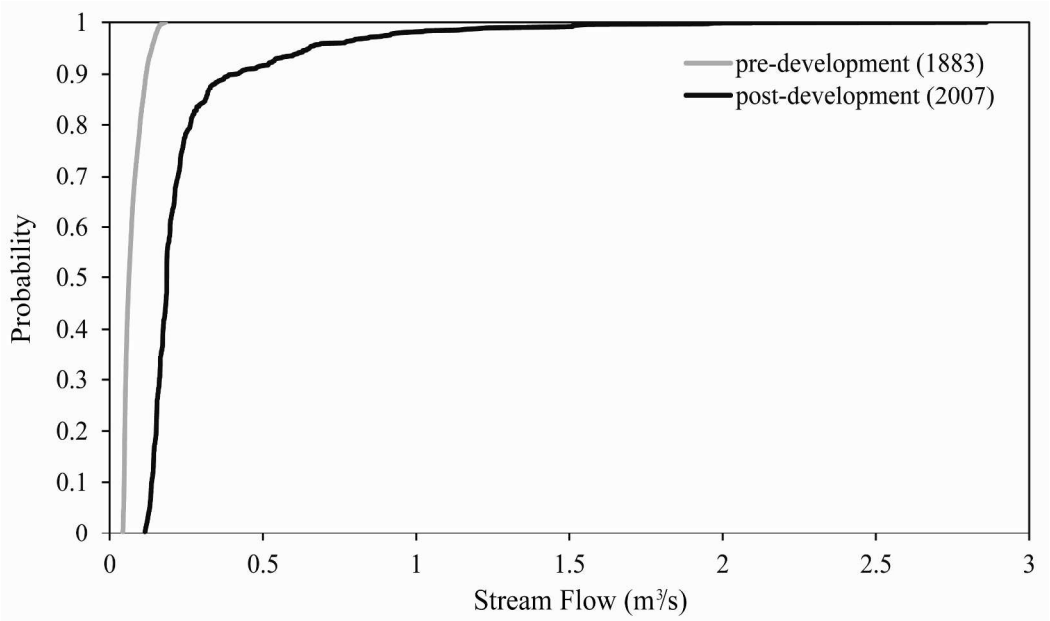

Fig. 8 Cumulative distribution function of mean daily summer streamflow from 2004 □ 2009 under the pre- (1883) and post-development (2007) scenarios

Peer Review

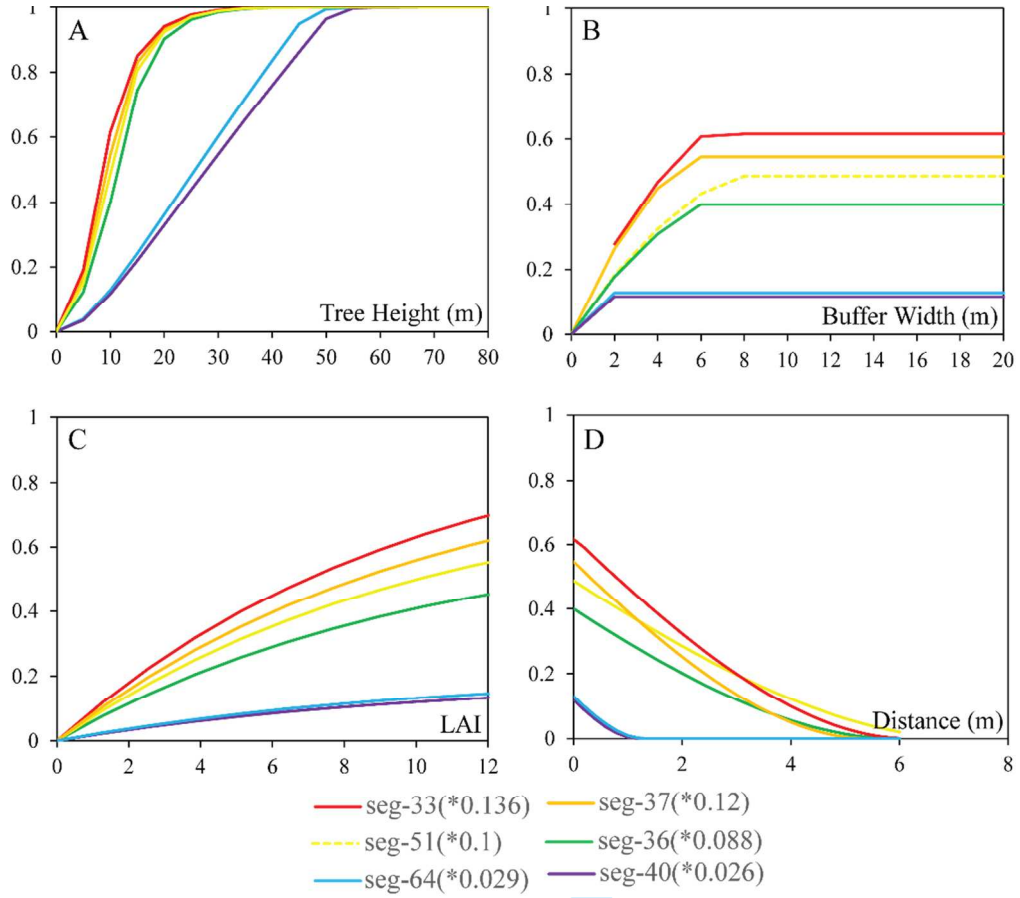

Fig. 9 Sensitivity of effective shading density (y-axis) to riparian vegetation parameters: (A) tree height, (B) buffer width, (C) LAI, and (D) bank to canopy distance given six selected segments at Mercer Creek. * indicates the index ratio of each segment

Review

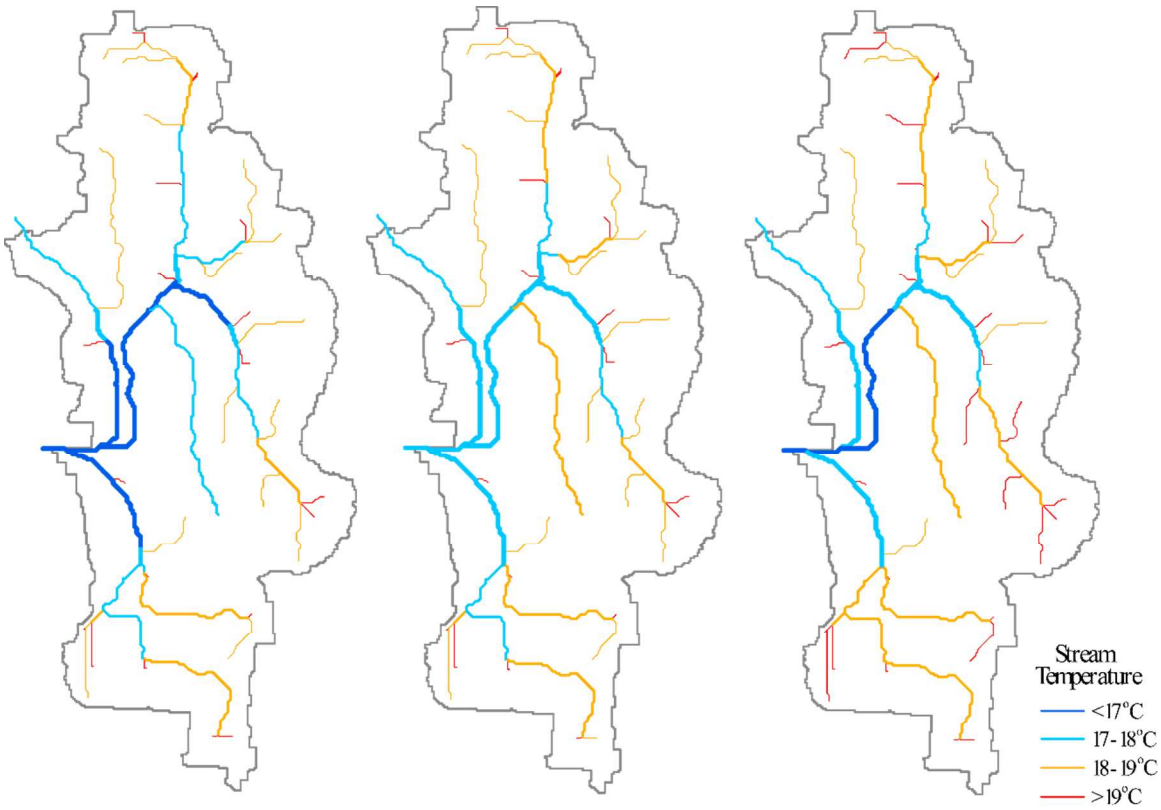

Fig. 10 Thermal map showing the annual maximum temperature for Mercer Creek. Thinner lines represent lower-order stream segment and thicker lines represent higher-order stream segments